# Bioconvection of negatively geotactic microorganisms in a porous medium: the effect of cell deposition and declogging

A.V. Kuznetsov and N. Jiang
*Department of Mechanical and Aerospace Engineering, North Carolina State University, Raleigh, NC, USA*

Received September 2001
Revised September 2002
Accepted October 2002

***Keywords*** *Convection, Porous media, Instability*

***Abstract*** *Mechanisms of deposition and declogging are considered while formulating a new continuum model for bioconvection in a dilute suspension of motile, negatively geotactic microorganisms in a porous medium. According to research in 1988, bioconvection is the name given to pattern-forming convective motions set up in suspensions of swimming microorganisms. "Negative geotaxis" means that the microorganisms tend to swim against the gravitational force. This paper is motivated by experimental research by Kessler who investigated the effect of porous media on the development of convection instability in algal suspensions. In the model suggested in this paper, the decrease of permeability due to cell adsorption by the porous medium is considered and the influence of this permeability decrease on the development of bioconvection is studied. The existence and stability of a two-dimensional plume in a rectangular enclosure with stress-free sidewalls is investigated. Governing equations include the Darcy law as well as the microorganism conservation equations. A conservative finite-difference scheme is utilized to solve these equations numerically. The analysis of the proposed model reveals that the major factors affecting the development of bioconvection are the initial permeability of the porous medium and the rate of cell deposition. For small permeability, the resistance to the fluid flow is too large, and bioconvection does not develop. If the rate of cell deposition is too large, the number of suspended cells quickly becomes too small because of cell capturing by the porous medium. For this reason, the critical density difference in the top fluid layer cannot be reached, and bioconvection does not develop.*

## Nomenclature

$c_a$ = acceleration coefficient
$d$ = average diameter of a particle constituting the porous matrix, m
$D$ = diffusion coefficient, $m^2/s$
$\mathbf{g}$ = gravity vector, $m/s^2$
$H$ = height of the enclosure, m
$\mathbf{J}$ = flux of the cells, $1/(m^2 s)$
$k_{dep}$ = rate of cell deposition, 1/s
$k_{decl}$ = rate of cell declogging, 1/s
$K$ = permeability, $m^2$
$L$ = width of the enclosure, m
$\bar{n}$ = total number of cells (captured plus suspended) in the enclosure over volume of the enclosure, cells/$m^3$
$n_c$ = number of captured cells per unit volume, $1/m^3$
$n_s$ = number of suspended cells per unit volume, $1/m^3$

AVK gratefully acknowledges the grant # NAG3-2706 awarded to him by NASA Office of Biological and Physical Research, Physical Sciences Division. Critical comments of Professor J.O. Kessler are also greatly appreciated.

International Journal of Numerical Methods for Heat & Fluid Flow
Vol. 13 No. 3, 2003
pp. 341-364

0961-5539
DOI 10.1108/09615530310464535

$n_c^*$ = dimensionless number of captured cells per unit volume, $n_c/\bar{n}$
$n_s^*$ = dimensionless number of suspended cells per unit volume, $n_s/\bar{n}$
$\bar{\mathbf{p}}$ = unit vector indicating the direction of cell swimming, $-\mathbf{g}/|\mathbf{g}|$
$P_e$ = excess pressure (above hydrostatic), Pa
$R_a$ = rate of cell deposition, $1/(m^3 s)$
$t^*$ = dimensionless time, $tD/L^2$
$\mathbf{v}$ = filtration velocity, m/s
$u$ = horizontal velocity component, m/s
$v$ = vertical velocity component, m/s
$W_c\bar{\mathbf{p}}$ = vector of average swimming velocity relative to the fluid ($W_c$ is assumed to be constant), m/s
$x$ = horizontal coordinate, m
$x^*$ = dimensionless width, $x/L$
$y$ = vertical coordinate, m
$y^*$ = dimensionless height, $y/L$

*Greek symbols*

$\Delta\rho$ = density difference, $\rho_{cell} - \rho_0$, $kg/m^3$
$\zeta$ = vorticity, 1/s
$\zeta^*$ = dimensionless vorticity, $\zeta L^2/D$
$\theta$ = average volume of the cell, $m^3$
$\mu$ = dynamic viscosity, assumed to be approximately the same as that of water, kg/(m s)
$\rho_0$ = density of water, $kg/m^3$
$\varphi$ = porosity of the medium
$\varphi_0$ = initial porosity of the medium (before any cells are adsorbed)
$\psi$ = stream function, $m^2/s$
$\psi^*$ = dimensionless stream function, $\psi/D$

## 1. Introduction

Microbiological fluid mechanics is one of the most vibrant areas of modern fluid dynamics. Most significant results in this area were obtained over the last two decades (Ghorai and Hill, 1999; Pedley and Kessler, 1987, 1990; Pedley *et al.*, 1988). Unlike traditional multiphase flow mechanics, where solid particles are passive and are either carried by the fluid flow or pushed by external forces, such as buoyancy (in sedimentation problems), microbiological fluid mechanics considers the flow of self-propelled microorganisms, such as motile species of bacteria and algae. These microorganisms swim by rotating flagella driven by reversible molecular motors that are embedded in the cell wall (Berg, 1975). The bacterial flagellar motor is a rotary engine that derives its energy from the electrochemical gradient established between the cell cytoplasm and the periplasmic lumen. This gradient drives an ion flow through the motor, which is then transduced into a rotary torque. When the motor rotates counterclockwise, the helical flagella propagate a wave from the cell body. This causes the adjacent flagella to intervene and form a propulsive corkscrew that drives the bacterium through the fluid medium at speeds of up to 25 $\mu$m/s (Anderson, 1975; Childress, 1981). In many cases, the molecular motor periodically reverses its direction of rotation, producing, on average, irregular locomotion towards some specific direction. The number of these self-propelled microorganisms in 1 $cm^3$ of suspension may be very large (about $10^7$ for a dilute regime and up to about $10^{11}$ for a close packed (turbulent) regime) and the flow pattern can be very complex.

Bioconvection is the term used to describe the phenomenon of spontaneous pattern formation in suspensions of motile microorganisms (Kessler, 1985a, b; Pedley and Kessler, 1992). In this paper, a dilute suspension of negatively geotactic microorganisms in a fluid saturated porous medium is considered.

*Negative geotaxis* means that microorganisms tend to swim against the gravitational force (Childress *et al.*, 1975). This behavior is typical for many motile species of microorganisms, such as protozoa *Tetrahymena pyriformis*, considered by Childress *et al.* (1975), and motile algal species *Dunaliella*, *Chlamydomonas nivalis*, and *Chlamydomonas rosae*, considered by Kessler (1986). It should be noted that negative geotaxis is a model used to describe the behavior of certain species of microorganisms. As any model, it is an approximation of a real life phenomenon. For algal suspensions, *gyrotaxis* (Pedley *et al.*, 1988), which accounts for deviation from a strictly upward direction of swimming caused by vorticity of bioconvection-induced flow, may be a better approximation. However, negative geotaxis is a valid well-tested model, utilized, for example, by Childress *et al.* (1975). Gyrotactic reorientation of swimming direction has also been ignored in a recent paper by Metcalfe and Pedley (2001). For these reasons, in this paper, it is assumed that microorganisms exhibit simple upswimming, the negative geotaxis.

Negative geotaxis causes concentration of microorganisms in the upper portion of the enclosure. Due to the higher concentration of microorganisms, the density of the top fluid layer increases, and once it becomes larger than the critical value, the fluid structure becomes unstable resulting in the development of an overturning instability. This is similar to the Rayleigh-Benard convection instability but its development does not require a temperature gradient.

Despite the considerable number of publications on bioconvection, there is a lack of research in bioconvection in porous media. Bioconvection in porous media may be an important phenomenon in many applications. Kessler (1986) suggested the utilization of upswimming algal cells to concentrate the cells, purify cultures, and to separate vigorously swimming subpopulations. Utilizing upswimming, it is also possible to separate dead and alive cells. For these applications, bioconvection is undesirable, because it would prevent upswimming cells from concentrating near the surface of the culture. In experiments carried out by Kessler (1986), a porous medium (a surgical cotton wool) was utilized to suppress bioconvection. According to Kessler (1986), the porous medium must satisfy two requirements; it must be sufficiently permeable to allow cells to swim through it but also sufficiently tight to damp out bioconvection. For practical purposes, it is desirable to have the permeability of the porous medium as high as possible (otherwise, the microorganisms may cut their tails off while swimming through the porous medium). Also, having the permeability as high as possible maximizes the flux of the cells in the upward direction and reduces the duration of the process.

Understanding the motion of microorganisms in a porous medium is also a key to understanding and controlling some technological and industrial processes such as microbial-enhanced oil recovery (Kim and Fogler, 2000; Stewart and Fogler, 2001). Bioconvection in porous media is a complex, dynamic process. In a porous medium, the transport of cells is different from

that in a homogeneous fluid. The swimming microorganisms may be adsorbed by the porous medium. A fraction of the adsorbed cells may be released to return back into the suspension through the declogging process. The accumulation of cells in the porous matrix leads to a decrease in permeability of the porous medium. This permeability decrease affects the ability of cells to penetrate through microchannels in the porous matrix. Therefore, the adsorption of cells by the porous medium affects the development of bioconvection.

Pedley *et al.* (1988), formulated a continuum model of bioconvection in a suspension of motile gyrotactic microorganisms . This formulation includes the Navier-Stokes equations for an incompressible fluid and the microorganism conservation equation. Using the continuum model of Pedley *et al.* (1988), Ghorai and Hill (1999, 2000) introduced a stream function-vorticity formulation, which makes the problem more suitable for numerical solution techniques. Cases with different initial conditions and different width-to-height ratios of a deep enclosure were compared.

Corapcioglu and Haridas (1984, 1985) presented a theoretical investigation of transport and accumulation of microorganisms in a porous medium and suggested a numerical model for microbial transport in soils and groundwater. The deposition and declogging mechanisms were considered in their model.

This paper focuses on the analysis of bioconvection development in a suspension of negatively geotactic microorganisms in a porous medium. This is different from Kuznetsov and Jiang (2001), because cell deposition and declogging are accounted for in the present investigation. The suspension is assumed to be dilute and the Darcy law is utilized to formulate the momentum equation to describe the filtration of this suspension in a porous medium. This problem is somewhat similar to natural convection in a porous layer heated from below (Nield and Bejan, 1999). The difference is that in bioconvection there is no temperature gradient. It is the upswimming of the microorganisms that induces density gradient in the fluid.

## 2. Mathematical formulation

### *2.1 Governing equations*

A two-dimensional porous rectangular enclosure of width $L$ and height $H$ is considered. The walls are impermeable, which means no flux of the cells is permitted through any of the walls.

The model is based on the assumption that the length scales of bulk motions and concentration distributions are large when compared to the cell diameter and typical cell spacing. Inertia is also neglected when the dynamics of a cell's motion relative to the fluid is described. The suspension is assumed to be dilute, i.e. it is assumed that the volumetric cell concentration is much smaller than unity, $\bar{n}\theta \ll 1$.

It is also assumed that the cells swim with a known constant relative velocity. The cells are assumed to be symmetrical so that they experience no force in a pure straining motion. This problem is governed by the following differential equations:

*Conservation of mass*

It is assumed that the suspension is incompressible:

$$\nabla \cdot \mathbf{v} = 0 \tag{1}$$

where $\mathbf{v}$ is the filtration velocity.

*Conservation of momentum*

The momentum equation for the suspension is formulated utilizing the Darcy law and the Boussinesq approximation:

$$c_a \rho_0 \frac{\partial \mathbf{v}}{\partial t} = -\nabla P_e - \frac{\mu}{K}\mathbf{v} + n_s \theta \Delta\rho \mathbf{g} \tag{2}$$

where $c_a$ is the acceleration coefficient introduced by Nield and Bejan (1999), this coefficient depends sensitively on the geometry of the porous medium; $\rho_0$ the density of water; $\theta$ volume of the cell; $n_s$ the number of suspended cells per unit volume; $P_e$ the excess pressure (above hydrostatic); $K$ the permeability; $\mu$ the dynamic viscosity, which is assumed to be approximately the same as that of water; $\Delta\rho$ equals ($\rho_{cell} - \rho_0$); and $\mathbf{g}$ is the gravity vector.

The permeability of the porous medium, $K$, is calculated utilizing the Carman-Kozeny model that results in the following dependence of the permeability on porosity (Nield and Bejan, 1999):

$$K = \frac{d^2(1-\varphi)^3}{180\varphi^2} \tag{3}$$

where $d$ is the average diameter of a particle constituting the porous matrix. The porosity of the medium, $\varphi$, is calculated as:

$$\varphi = \varphi_0 - n_c \theta \tag{4}$$

where $\varphi_0$ is the initial porosity of the medium (before any microorganisms are adsorbed) and $n_c$ is the number of captured cells per unit volume.

Equations (3) and (4) enable coupling clogging and declogging processes with the momentum transfer in porous media.

Equation (2) is derived by utilizing the Boussinesq approximation and neglecting all effects of the cells on the fluid (except their negative buoyancy) because the suspension is dilute. For the numerical solution, equation (2) is recast in terms of vorticity by taking the curl of both sides of this equation:

$$c_a \rho_0 \frac{\partial \zeta}{\partial t} = -\frac{\mu}{K}\zeta - \theta \Delta\rho g \frac{\partial n_s}{\partial x} \tag{5}$$

where $\zeta$ is the vorticity and $x$ is the horizontal coordinate.

*Conservation of suspended cells*

The total number of cells in the enclosure is assumed to be constant (the cells do not die or multiply), which is reasonable because the time scale for the development of bioconvection is much smaller than the time scale of cells' metabolism. This assumption results in the following equation of conservation of suspended cells, which is obtained by modifying equation (2.5) of Pedley *et al.* (1988) to account for cell deposition:

$$\frac{\partial(n_s)}{\partial t} = -\nabla \cdot \mathbf{J} - R_a \tag{6}$$

where $\mathbf{J} = n_s \mathbf{v} + n_s W_c \bar{\mathbf{p}} - D\nabla n_s$ is the flux of suspended cells, $R_a = (k_{dep} n_s - k_{decl} n_c)$ is the rate of cell deposition, $W_c \bar{\mathbf{p}}$ is the vector of average swimming velocity relative to the fluid ($W_c$ is assumed to be constant), $\bar{\mathbf{p}}$ is the unit vector indicating the direction of cell swimming, and $D$ is the diffusion coefficient.

*Conservation of deposited cells*

The equation of conservation of deposited cells is:

$$\frac{\partial n_c}{\partial t} = R_a \tag{7}$$

The stream function, $\psi$, and the vorticity, $\zeta$, are defined as:

$$u = \frac{\partial \psi}{\partial y}, \quad v = -\frac{\partial \psi}{\partial x}, \quad \zeta = -\nabla^2 \psi \tag{8}$$

The width $L$, the time scale $L^2/D$, and the mean concentration $\bar{n}$ are used as the reference values in these equations. The resulting system of coupled differential equations is:

$$\zeta^* = -\frac{\partial^2 \psi^*}{\partial x^*} - \frac{\partial^2 \psi^*}{\partial y^*} \tag{9}$$

$$\frac{\partial \zeta^*}{\partial t^*} = -\frac{\mu L^2}{DKc_a \rho_0} \zeta^* - \frac{\theta \Delta \rho g L^3 \bar{n}}{D^2 c_a \rho_0} \frac{\partial n_s^*}{\partial x^*} \tag{10}$$

$$\frac{\partial n_s^*}{\partial t^*} = -\nabla \mathbf{J}^* - R_a^* \tag{11}$$

$$\mathbf{J}^* = n_s^* \mathbf{v} + n_s^* W_c L \mathbf{p}/D - \nabla n_s^* \tag{12}$$

$$R_a^* = (L^2/D)(k_{dep} n_s^* - k_{decl} n_c^*) \tag{13}$$

and

$$\frac{\partial n_c^*}{\partial t^*} = R_a^* \tag{14}$$

In equations (9)-(14), the following dimensionless parameters are utilized:

$$\psi^* = \frac{\psi}{D}, \quad \zeta^* = \frac{\zeta L^2}{D}, \quad t^* = \frac{tD}{L^2}, \quad n_s^* = n_s/\bar{n}, \quad n_c^* = n_c/\bar{n}, \quad x^* = x/L, \quad y^* = y/L \tag{15}$$

*2.2 Initial and boundary conditions*

The computational domain is shown in Figure 1. The normal velocity components must vanish at the boundaries because the boundaries are impermeable. The normal component of the cell flux must also equal zero at the boundaries. A minor difficulty must be resolved at the free surface. At the free surface, the fluid vertical velocity, $v$, is zero. However, suspended cells at the free surface are swimming upwards. Therefore, to impose a no-cell-flux condition through the free surface the following condition, which follows from equation (12), must be satisfied:

$$n_s^* W_c L - D\frac{\partial n_s^*}{\partial y^*} = 0 \tag{15a}$$

Equation (15(a)) describes a diffusion polarization layer.

Since the Darcy law is utilized, the governing equations are of the first-order in the spatial derivatives. Therefore, only one condition for velocity components can be utilized at a given boundary. For this reason, other velocity components, except the component normal to the boundary, can take on an arbitrary

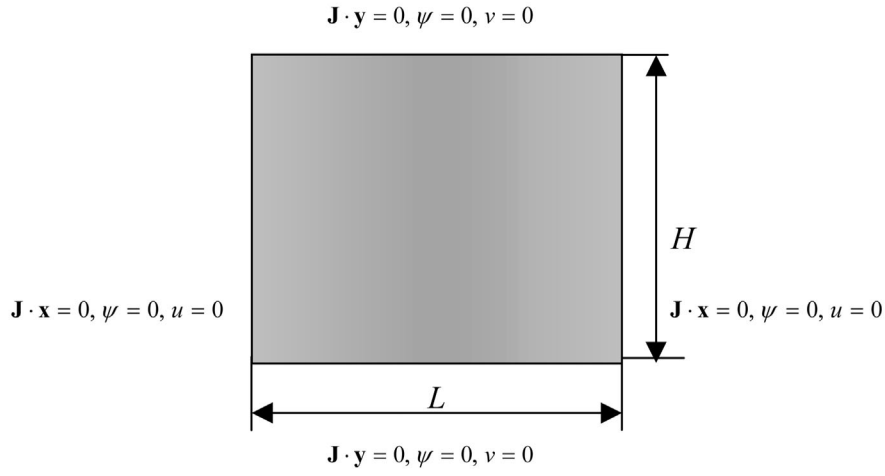


**Figure 1.**
Computational domain and boundary conditions

value at the boundary (Nield and Bejan, 1999). The boundary conditions utilized for this problem are:

$$x^* = 0 \text{ and } x^* = 1: \quad \mathbf{J}\cdot\mathbf{x} = 0, \quad \psi = 0, \quad u = 0 \tag{16}$$

$$y^* = 0 \text{ and } y^* = 1: \quad \mathbf{J}\cdot\mathbf{y} = 0, \quad \psi = 0, \quad v = 0 \tag{17}$$

Initially, a uniform cell distribution is assumed. However, to facilitate the numerical solution a small perturbation to the uniform concentration of suspended cells is utilized:

$$\psi = 0, \quad \zeta^* = 0, \quad n_s^* = 1 + \varepsilon\cos(m\pi x), \quad n_c^* = 0 \tag{18}$$

where $\varepsilon = 10^{-5}$ and $m = 2$. This perturbation is utilized for computational convenience to ensure that the plume forms in the middle of the enclosure.

*2.3 Numerical procedure*

A conservative finite-difference scheme is used to discretize the governing equations. An implicit scheme with Euler backward differencing in time and central differencing in space is utilized to obtain the transient solutions. A line-by-line tridiagonal matrix algorithm with relaxation is used together with an iteration technique to solve the nonlinear discretized equations. A uniform grid is utilized. To check the grid independence of the solutions, the solutions on different grids for the same enclosure are compared in Section.

## 3. Results and discussion

An enclosure whose depth equals its width is considered. In the beginning, the concentration of captured cells is equal to zero and all cells are swimming upwards. The parameter values utilized in these computations are summarized in Table I.

*3.1 The case of no cell deposition ($k_{dep} = k_{decl} = 0\,1/s$)*

First, the case of no cell deposition is considered. This means that no cells are captured by the porous medium and the permeability remains constant during the whole process of the development of bioconvection.

*3.1.1 A low-permeability case.* When the bioconvection is developing, the magnitude of vorticity, $\zeta^*$, must increase. Considering the situation when $\zeta^*$ is positive, $\frac{\partial \zeta^*}{\partial t^*}$ must be larger than zero. From equation (10) the following inequality is obtained:

$$-\frac{\theta\Delta\rho g L^3 \bar{n}}{D^2 c_a \rho_0}\,\frac{\partial n_s^*}{\partial x^*} > \frac{\mu L^2}{DKc_a\rho_0}\zeta^* \tag{19}$$

Since the physics of the problem requires that vorticity increases with time and $\zeta^*$ is positive, the right-hand side of the above expression must be larger than zero. Rearranging this equation, the following condition is obtained:

| Initial cell concentration | $\bar{n}$ | $10^{12}$ cells/m$^3$ |
|---|---|---|
| Density ratio | $\Delta\rho/\rho$ | 0.05 |
| Volume of the cell | $\theta$ | $5\times10^{-16}$ m$^3$ |
| Average swimming velocity | $W_c$ | $10^{-4}$ m/s |
| Diffusivity of cells | $D$ | $5\times10^{-8}$ m$^2$/s |
| Kinematic viscosity | $\nu$ | $10^{-6}$ m$^2$/s |
| Acceleration coefficient | $c_a$ | 1 |
| Height of the enclosure | $H$ | 0.005 m |
| Width of the enclosure | $L$ | 0.005 m |
| Initial porosity | $\varphi_0$ | 0.76 |
| Average diameter of a pore | $d$ | Figure 2: $8.7\times10^{-3}$ m<br>Figures 3-7: $8.7\times10^{-2}$ m<br>Figures 8 and 9: $7\times10^{-2}$ m |
| Initial permeability | $K_0$ | Figure 2: $10^{-8}$ m$^2$<br>Figures 3-7: $10^{-6}$ m$^2$<br>Figures 8 and 9: $6.5\times10^{-7}$ m$^2$ |

**Table I.**
Physical properties utilized in computations

$$-\frac{\partial n_s^*}{\partial x^*}\frac{1}{\zeta^*} > \frac{\mu D}{K\bar{n}L\theta\Delta\rho g} \tag{20}$$

This condition must always be satisfied in the development of bioconvection. Therefore, the permeability, $K$, is a very important parameter in modeling. It decides whether convection occurs or not. For a small permeability value (such as $10^{-8}$ m$^2$), bioconvection does not develop. The cells simply accumulate in the top fluid layer. No overturning instability occurs. The initial perturbation also vanishes as time passes.

Figure 2(a)-(c) displays dimensionless concentration of suspended cells (a), the streamline contours (b), and the total cell flux vectorfield **J** (c), respectively, at $t^* = 0.2$ when the permeability equals $10^{-8}$ m$^2$. The cell flux displayed in Figure 2(c) is mainly due to the diffusion of cells. The circulation shown in Figure 2(b) is very weak and is due to the initial perturbation of cell concentration given by the third equation in (18).

*3.1.2 A high-permeability case*. If permeability is $10^{-6}$ m$^2$, the development of bioconvection occurs. First, the concentration of cells in the top fluid layer increases while the concentration in the bottom fluid layer decreases. When $t^*$ approximately equals 0.1, a critical state is approached and the development of bioconvection begins.

Figure 3(a)-(c) shows the cell concentration (a), the streamline contours (b), and the total cell flux vectorfield **J** (c), respectively, right before the convection instability occurs (for $t^* = 0.101$). The concentration of cells in the center of the top fluid layer increases faster than at the sidewalls (the cells accumulate in the center of the top layer). Figure 3(a) shows that most of the cells have accumulated in the top layer. There is also a very weak symmetrical circulation

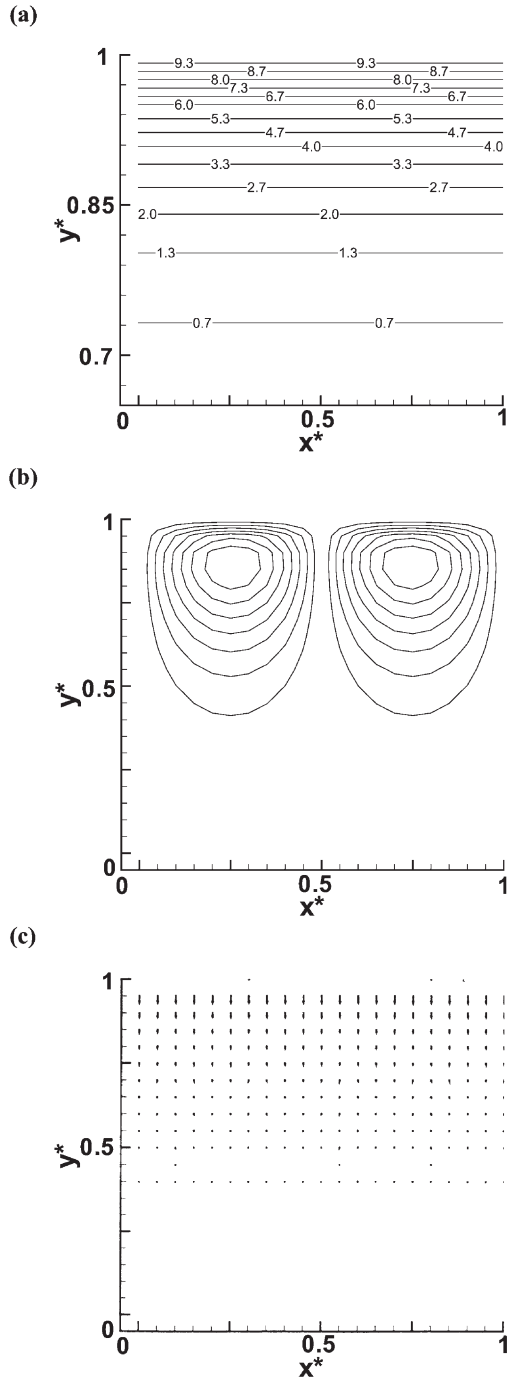


**Figure 2.**
The case of small permeability, $t^* = 0.2$: (a) dimensionless concentration of suspended cells, $n_s^*$, (b) streamlines, and (c) cell flux, **J**

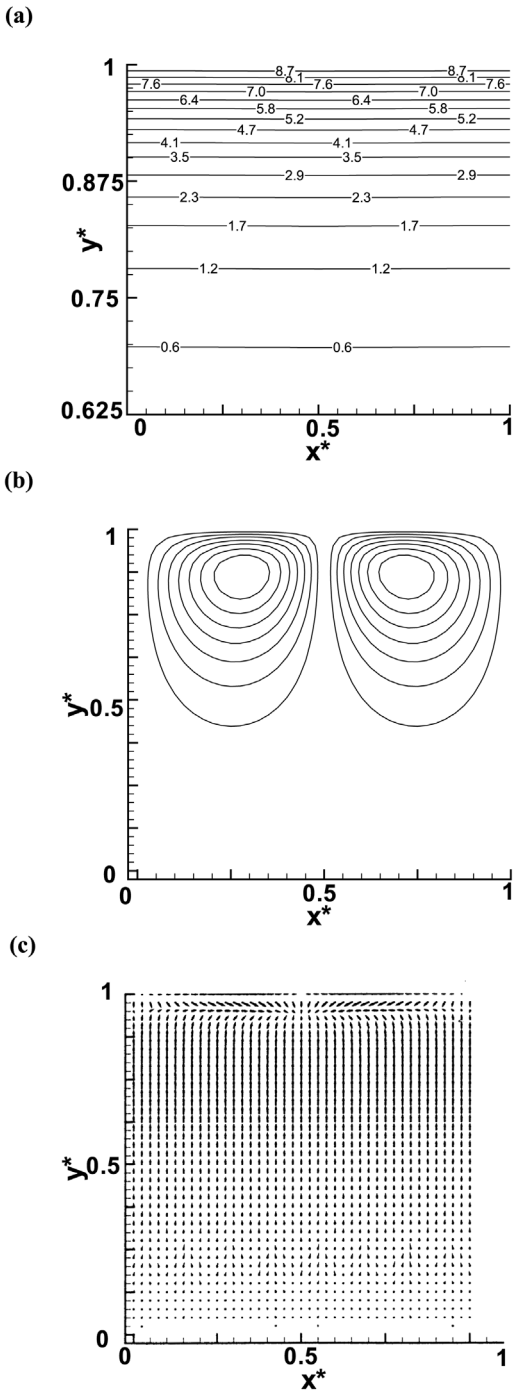


**Figure 3.**
The state right before the convection starts to develop, $t^* = 0.101$: (a) dimensionless concentration of suspended cells, $n_s^*$, (b) streamlines, and (c) cell flux, **J**

shown in Figure 3(b), which is due to the perturbation given to the initial uniform concentration. Because most of the cells are in the top layer, the cell flux at the bottom is very small while it is very large near the top of the enclosure. The flux due to convection is still very small at this time. In the top layer, because of the small initial perturbation, the cells are moving to the center.

Figure 4(a)-(c) shows how the plume starts to develop. These figures are computed for $t^* = 0.128$. In the beginning stage of plume development, the concentration of cells in the center of the top fluid layer increases more rapidly than at the sidewalls. This results in a larger concentration of cells in the center compared to that at the sidewalls as shown in Figure 4(a). This occurs because the cells move to the center due to the initial perturbation; the number of cells that move upward decreases because most of the cells have already accumulated in the top layer. Figure 4(c) shows that the horizontal component of the total cell flux in the top layer continuously increases. This means that the contribution of convection in the total cell flux is getting larger.

Figure 5(a)-(c) shows the cell concentration (a), the streamline contours (b), and the total cell flux vectorfield **J** (c) right before the head of the plume begins to descend, for $t^* = 0.147$. As the cells accumulate in the center of the top layer, the flux due to diffusion increases. While convection develops, the velocity of the fluid becomes larger. Due to the above two reasons, the cells in the center of the top layer are carried downward by convection more quickly than for the moment of time shown in Figure 4(a)-(c). Therefore, the rate of cell accumulation in the center of the top layer becomes smaller. This indicates that convection is attaining its steady-state.

Figure 6(a)-(c) shows the steady-state of this process, when $t^* > 0.3$. In numerical computations, the steady-state is defined as follows: the maximum relative change of the concentration of cells among all grid points is less than $10^{-6}$. At steady-state, the circulation almost hits the bottom of the enclosure. The flux due to upswimming of the cells is very small compared to the flux due to macroscopic motion of the fluid. The contribution of upswimming into the total cell flux is very different from that in the beginning of the process, when the change of concentration of cells was mainly due to their upswimming.

To check the grid independence of the solution, computations for different grid sizes are performed. Computational results for $31 \times 31$ and $41 \times 41$ grids are found to be almost identical, proving the grid independence of the solution.

### *3.2 A case of moderate rates of cell deposition and declogging ($k_{dep} = 6.5 \times 10^{-4}$ 1/s, $k_{decl} = 4.35 \times 10^{-4}$ 1/s)*

In this case, the effects of cell deposition and declogging are included. The number of captured cells is small, and some of the captured cells escape due to the declogging mechanism; therefore, the development of bioconvection is not

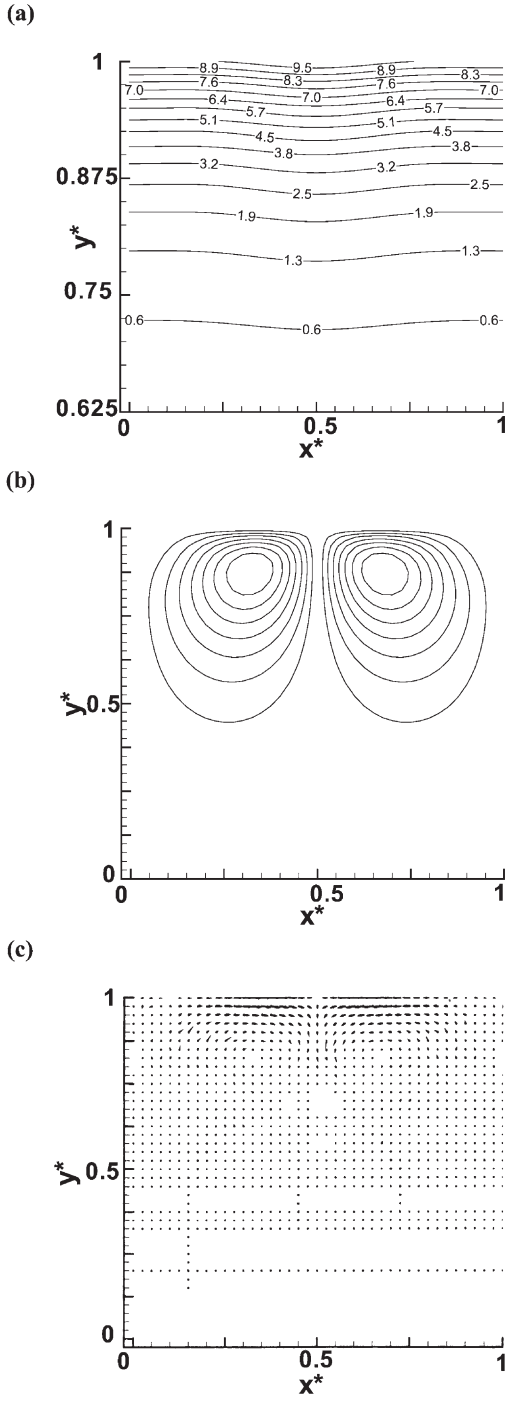


**Figure 4.**
Beginning of the development of convection, $t^* = 0.128$: (a) dimensionless concentration of suspended cells, $n_s^*$, (b) streamlines, and (c) cell flux, **J**

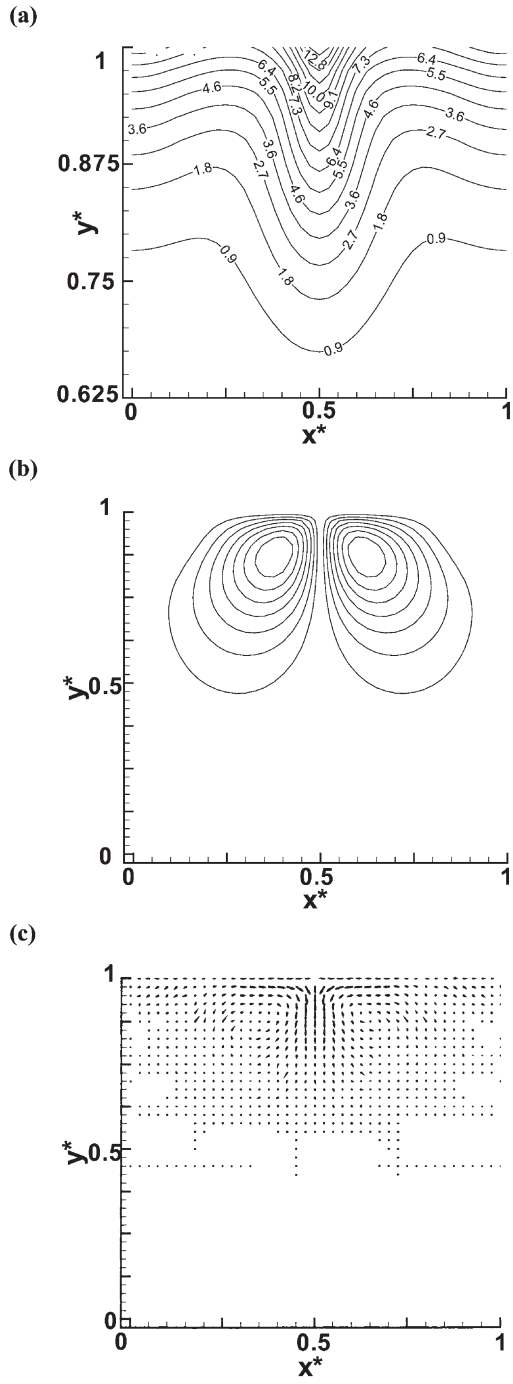


**Figure 5.**
The state right before the convection is developed, $t^* = 0.147$:
(a) dimensionless concentration of suspended cells, $n_s^*$,
(b) streamlines, and
(c) cell flux, **J**

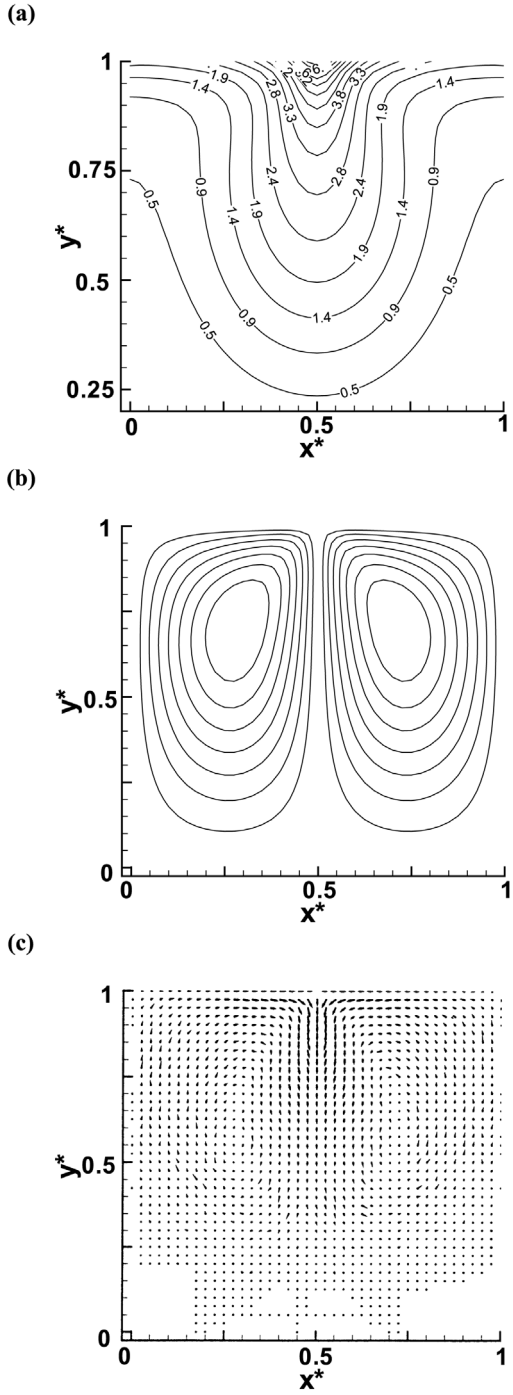


**Figure 6.**
Steady-state plume, $t^* > 0.3$: (a) dimensionless concentration of suspended cells, $n_s^*$, (b) streamlines, and (c) cell flux, **J**

considerably affected. The whole process is similar to that when the deposition and declogging mechanisms are ignored except some cells are being captured. Eventually, the process will reach its steady-state.

Figure 7(a) shows the concentration of suspended cells when bioconvection reaches its steady-state. Figure 7(b) displays the concentration of captured cells and Figure 7(c) depicts the streamlines. Concentration of suspended cells is approximately six times larger than concentration of captured cells, which shows that only a small portion of cells is captured. Concentration of both captured and suspended cells is the largest near the free surface in the center of the plume, as expected.

*3.3 A case of cell deposition only, the declogging mechanism is turned off* ($k_{dep} = 9.5 \times 10^{-4}$ *1/s,* $k_{decl} = 0$ *1/s)*

In this computation, the deposition mechanism is considered but the declogging mechanism is turned off. Therefore, the number of captured cells continuously increases during the whole process. In the beginning, bioconvection starts to develop because the number of captured cells is small and condition (20) is satisfied. This means that the time scale for the development of bioconvection is smaller compared to the time scale for cell deposition. As more and more suspended cells are captured, condition (20) fails, and bioconvection starts to decay. Eventually all cells will be captured.

Figure 8(a) shows the concentration of captured cells at $t^* = 0.4$, 2.4, and 3.4. The concentration continuously increases. Figure 8(b) shows the concentration of suspended cells at $t^* = 0.4$, 2.4, and 3.4. When $t^* = 0.4$, bioconvection plume has already developed. However, the concentration of suspended cells in the whole domain continues to decrease. Figure 8(c) shows the vorticity at $t^* = 0.4$, 2.4, and 3.4. The vorticity decreases after bioconvection plume has developed. It will asymptotically approach zero as time increases. This means that bioconvection will eventually disappear. Figure 8(d) displays the streamlines at $t^* = 0.4$, 2.4, and 3.4, respectively. The depth occupied by the plume is getting smaller because more and more cells are being captured.

*3.4 A case of large rate of cell deposition (*$k_{dep} = 6.5 \times 10^{-3}$ *1/s,* $k_{decl} = 4.35 \times 10^{-4}$ *1/s)*

If the rate of cell deposition is too large, most of the cells will be captured before bioconvection has a chance to develop. Thus the condition (20) fails before bioconvection plume develops. This means that the time scale for the development of bioconvection is larger compared to the time scale for cell deposition. Bioconvection plume will not develop. Instead, most of the cells will stay in the top fluid layer and most of them will be captured cells.

Figure 9(a) and (b) shows the concentration of the suspended cells and captured cells, respectively, for $t^* = 0.36$. Bioconvection does not develop. The concentration of captured cells is much larger than the concentration of

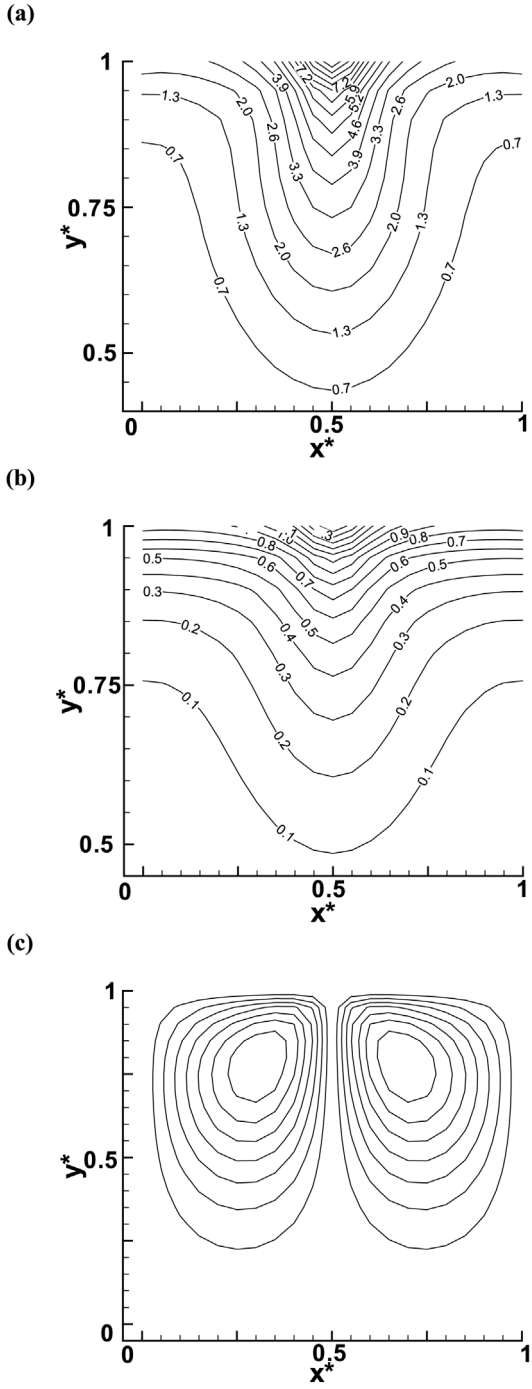


**Figure 7.**
A case of moderate rates of cell deposition and declogging ($k_{dep}=6.5\times10^{-4}$ 1/s, $k_{decl}=4.35\times10^{-4}$ 1/s), steady-state plume, $t^*>0.5$: (a) dimensionless concentration of suspended cells, $n_s^*$, (b) dimensionless concentration of captured cells, $n_c^*$, and (c) streamlines

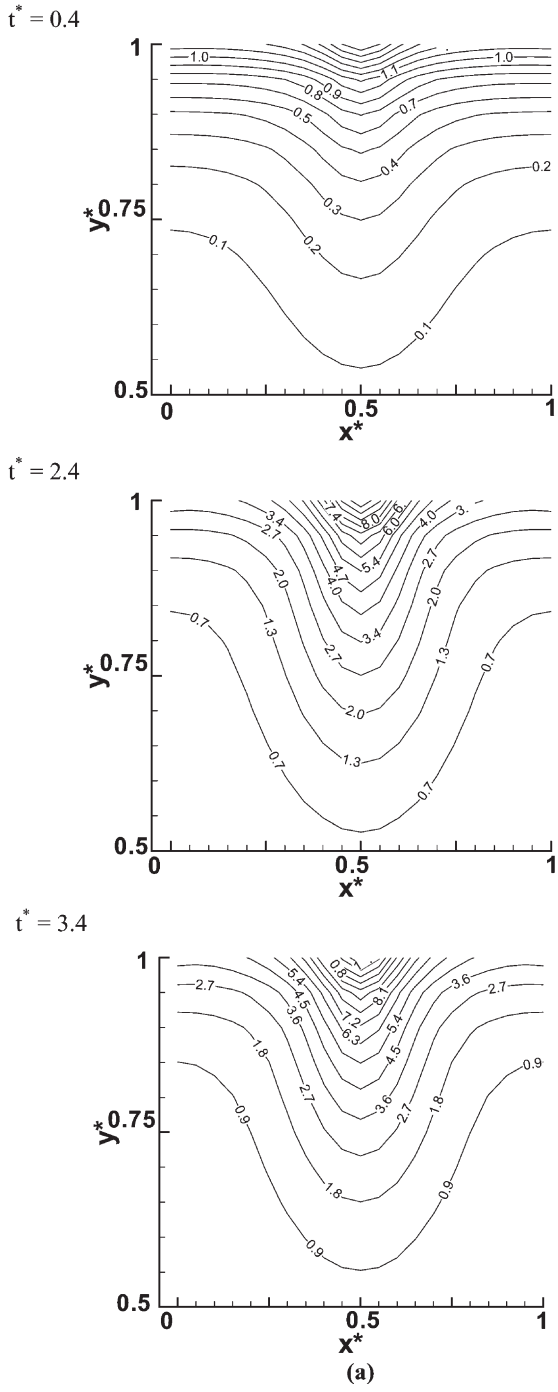


**Figure 8.**
A case of cell deposition only, the declogging mechanism is turned off ($k_{dep} = 9.5 \times 10^{-4}$ 1/s, $k_{decl} = 0$ 1/s):
(a) dimensionless concentration of captured cells, $n_c^*$,
(b) dimensionless concentration of suspended cells, $n_s^*$,
(c) dimensionless vorticity at $t^* = 0.4$, 2.4, and 3.4, and
(d) streamlines

*(Continued)*

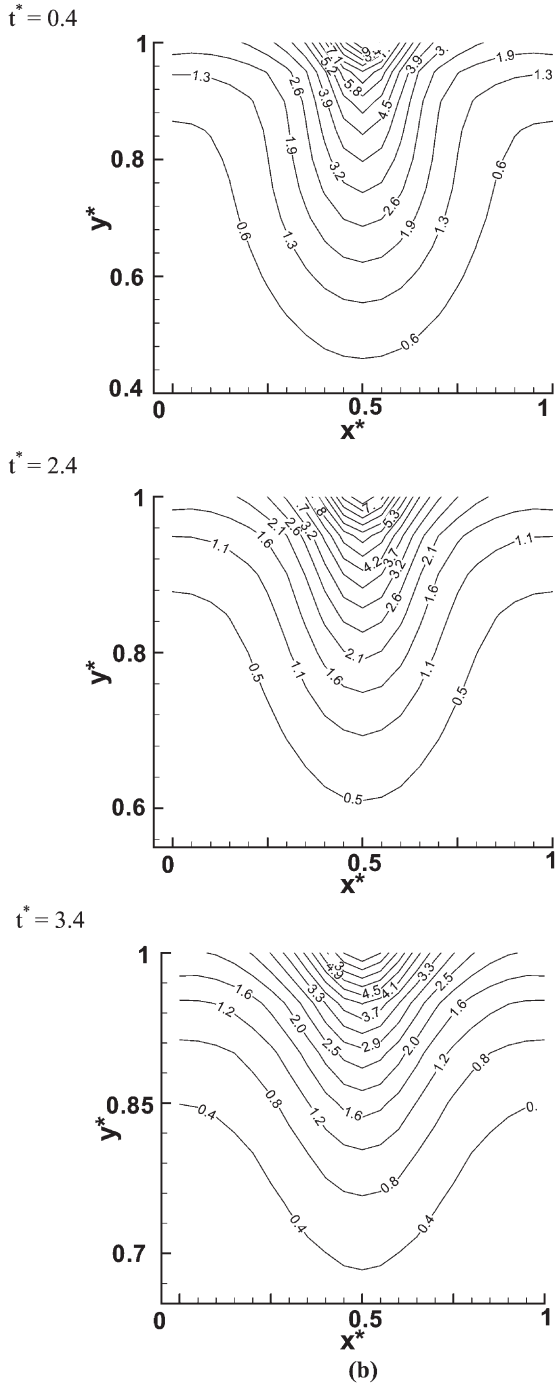


(b)

*(Continued)*

**Figure 8.**

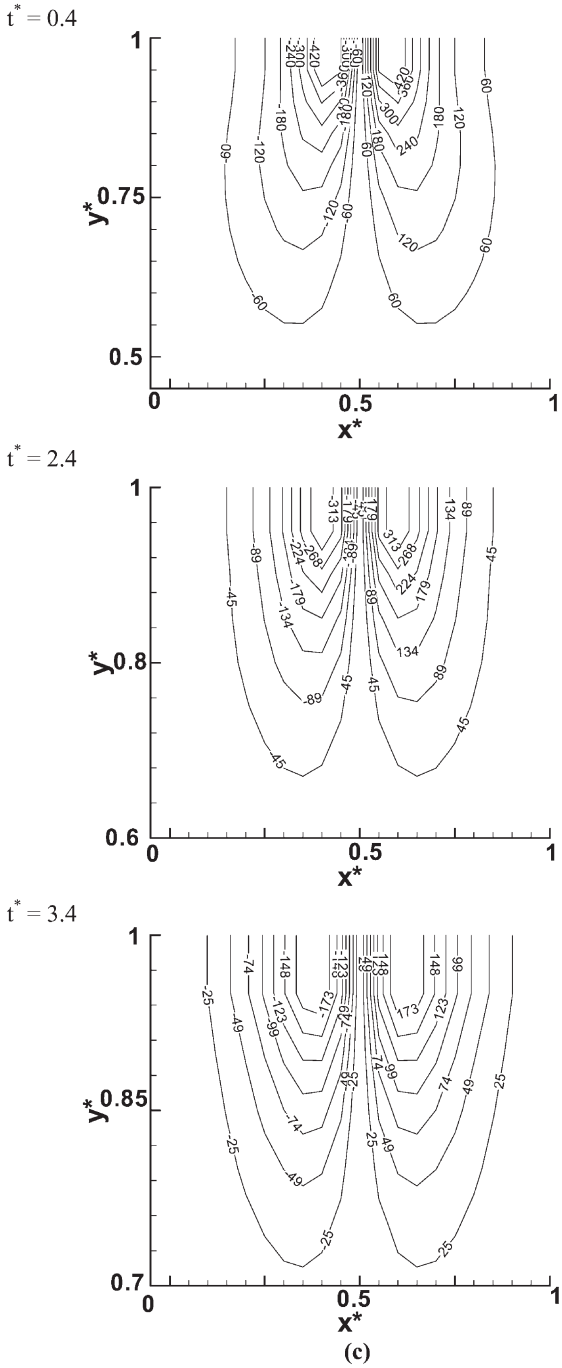


**Figure 8.**

*(Continued)*

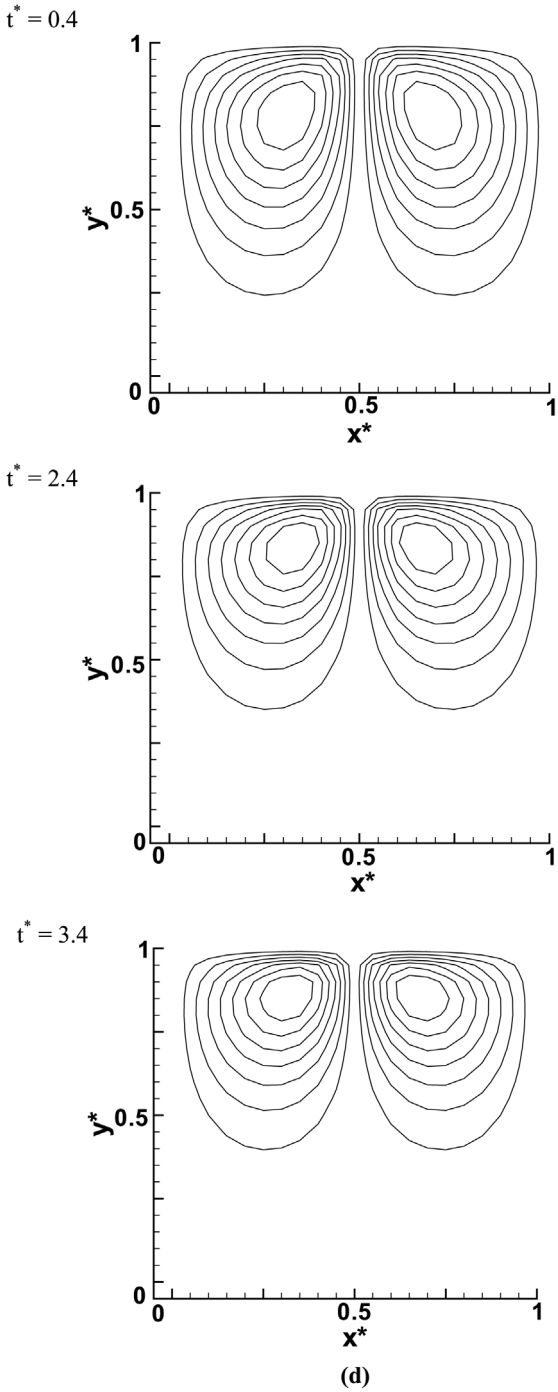


(d)

Figure 8.

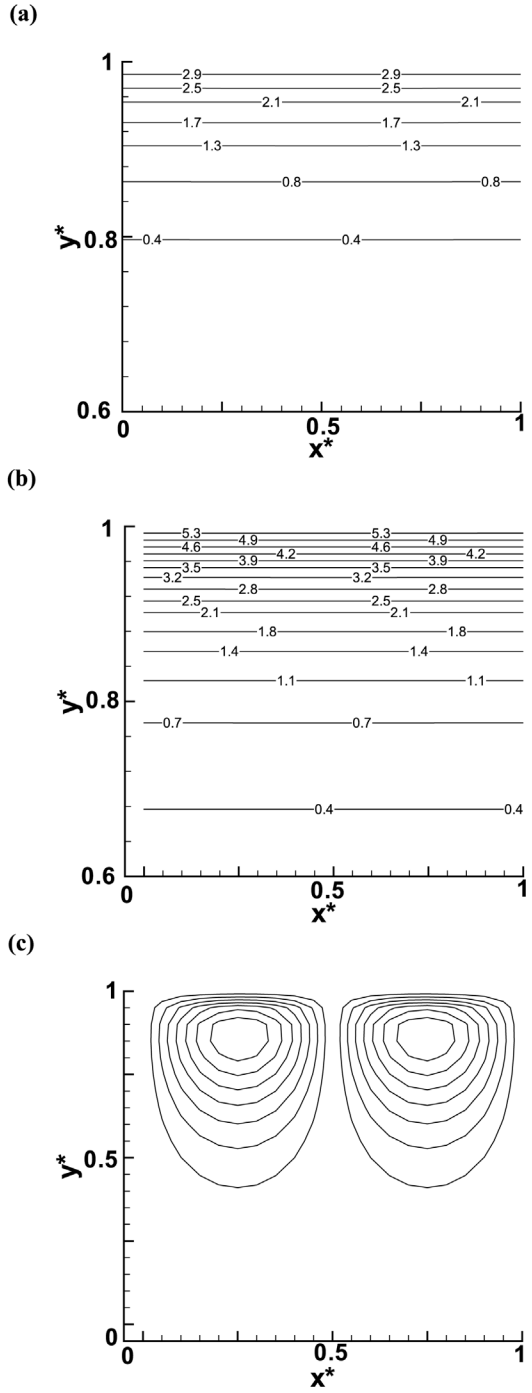


**Figure 9.**
A case of large rate of cell deposition ($k_{dep} = 6.5 \times 10^{-3}$ 1/s, $k_{decl} = 4.35 \times 10^{-4}$ 1/s), $t^* = 0.36$: (a) dimensionless concentration of suspended cells, $n_s^*$, (b) dimensionless concentration of captured cells, $n_c^*$ and (c) streamlines

the suspended cells. Figure 9(c) displays the streamlines. Similar to Figure 2(b), the circulation shown in Figure 9(c) is very weak and is caused by the initial perturbation of cell concentration.

## 4. Conclusions

This paper presents the first attempt to develop a model of bioconvection in a porous medium, which accounts for cell deposition and declogging. The analysis of this model reveals that there are several factors that affect the development of bioconvection. One of these factors is permeability. For small permeability, the resistance to the fluid flow is too large and bioconvection cannot develop. Another important factor in the development of bioconvection is the rate of cell deposition. Bioconvection develops because of the density difference between the microorganisms and the water. If the rate of cell deposition is too large, the critical density difference in the top fluid layer cannot be reached, and bioconvection does not develop.

### References

Andreson, R. (1975), "Formation of the bacterial flagellar bundle", in Wu, T., Brokaw, C. and Brennen, C. (Eds), *Swimming and Flying in Nature*, Plenum, New York.

Berg, H.C. (1975), "Chemotaxis in bacteria", *Annual Review of Biophysics and Bioengineering*, Vol. 4, pp. 119-36.

Childress, S. (1981), *Mechanisms of Swimming and Flying*, Cambridge University Press, Cambridge.

Childress, S., Levandowsky, M. and Spiegel, E.A. (1975), "Pattern formation in a suspension of swimming microorganisms: equations and stability theory", *J. Fluid Mech.*, Vol. 63, pp. 591-613.

Corapcioglu, M.Y. and Haridas, A. (1984), "Transport and fate of microorganisms in porous media: a theoretical investigation", *Journal of Hydrology*, Vol. 72, pp. 149-69.

Corapcioglu, M.Y. and Haridas, A. (1985), "Microbial transport in soils and groundwater: a numerical model", *Adv. Water Resources*, Vol. 8, pp. 188-200.

Ghorai, S. and Hill, N.A. (1999), "Development and stability of gyrotactic plumes in bioconvection", *J. Fluid Mech.*, Vol. 400, pp. 1-31.

Ghorai, S. and Hill, N.A. (2000), "Periodic arrays of gyrotactic plumes in bioconvection", *Physics of Fluids*, Vol. 12, pp. 5-22.

Kessler, J.O. (1985a), "Hydrodynamic focusing of motile algal cells", *Nature*, Vol. 313, pp. 218-20.

Kessler, J.O. (1985b), "Co-operative and concentrative phenomena of swimming microorganisms", *Contemp. Phys.*, Vol. 26, pp. 147-66.

Kessler, J.O. (1986), "The external dynamics of swimming micro-organisms", *Progress in Psycological Research*, Biopress, Bristol, Vol. 4, pp. 257-307.

Kim, D-S. and Fogler, H.S. (2000), "Biomass evolution in porous media and its effects on permeability under starvation conditions", *Biotechnology and Bioengineering*, Vol. 69, pp. 47-56.

Kuznetsov, A.V. and Jiang, N. (2001), "Numerical investigation of bioconvection of gravitactic microorganisms in an isotropic porous medium", *International Communications in Heat and Mass Transfer,* Vol. 28, pp. 877-886.

Metcalfe, A.M. and Pedley, T.J. (2001), "Falling plumes in bacterial bioconvection", *Journal of Fluid Mechanics*, Vol. 445, pp. 121-49.

Nield, D.A. and Bejan, A. (1999), *Convection in Porous Media*, 2nd edn., Springer-Verlag, New York.

Pedley, T.J. and Kessler, J.O. (1987), "The orientation of spheroidal microorganisms swimming in a flow field", *Proc. R. Soc. Lond.*, Vol. B231, pp. 47-70.

Pedley, T.J. and Kessler, J.O. (1990), "A new continuum model for suspensions of gyrotactic micro-organisms", *Journal of Fluid Mechanics*, Vol. 212, pp. 155-82.

Pedley, T.J. and Kessler, J.O. (1992), "Hydrodynamic phenomena in suspensions of swimming microorganisms", *Ann. Rev. Fluid Mech.*, Vol. 24, pp. 313-58.

Pedley, T.J., Hill, N.A. and Kessler, J.O. (1988), "The growth of bioconvection patterns in a uniform suspension of gyrotactic microorganisms", *J. Fluid Mech.*, Vol. 195, pp. 223-338.

Stewart, T.L. and Fogler, H.S. (2001), "Biomass plug development and propagation in porous media", *Biotechnology and Bioengineering*, Vol. 72, pp. 353-63.